Effect of particle shape on behaviour of sand in direct simple shear

A.W. Bezuidenhout
University of the Witwatersrand, Johannesburg, South Africa

ABSTRACT: Particle shape is widely considered to comprise three multi-scale descriptors that affect the mechanical behaviour of soil that include form, angularity and roughness. Form measures the overall aspect ratio, angularity the mesoscopic degree of the sharpness of corners and edges and roughness, the micro-scale surface irregularities of a soil particle. This work characterises and correlates the behaviour of angular to rounded saturated soils exhibiting dilative and contractive responses, in simple shear, to particle shape descriptors which are measured using focus variation microscopy principles. Characterisation of dilative and contractive soils is informed by the compression measured during consolidation and, most importantly, by the undrained shear strength, including the indirect measurement of shear induced pore water pressure generated during constant volume simple shear tests. Results show that an increase in particle angularity and irregularity correlates to an increase in friction angle, compressibility and large strain undrained shear stiffness. The work highlights the importance of particle shape on the undrained response of saturated contractive and dilative sands. Particle shape descriptors not only reflect the history of a soil but also influences in the global behaviour of a soil from particle packing to stiffness and shear strength.

1 INTRODUCTION

Particle shape commonly comprises three multi-scale descriptors (Fig. 1) influencing a soil's mechanical behaviour that include form, angularity, and roughness. Form measures aspect ratio, angularity (or conversely referred to as roundness) is a measure of the degree of sharpness of corners and edges, and roughness reflects microscopic surface irregularities (Janoo 1998, Clayton et al. 2009, Wang et al. 2020). These descriptors are widely considered independent because each can vary widely without influencing the others (Barrett 1980, Le Pen et al. 2013).

The nature of sand-sized particles limits techniques that involve manual measurement using a vernier calliper or ruler and laser scanning to measure particle geometry. This necessitates the measurement of particle geometry using photographic-based techniques such as high-resolution photography (Wang et al. 2020), automated imaging (Clayton et al. 2009), focus variation microscopy (Bezuidenhout 2023, Bezuidenhout et al. 2024) and X-ray microcomputed tomography (Alshibli et al. 2014; Zhao et al. 2015; Zhou et al. 2017) on coarse to fine-grained sands.

Particle shape is important to geotechnical engineering researchers and practitioners because it affects a soil's mechanical behaviour - highlighting the importance of correlation of particle shape descriptors to mechanical behavioural parameters. Holtz & Kovacs (1981) studied the effects of void ratio, angularity, surface roughness, and moisture content, amongst other parameters, on the mechanical behaviour of aggregates. They concluded that an increase in the friction angle correlated with increases in particle angularity and surface roughness. It is expected that smooth and rounded particles promote interparticle sliding behaviour, whereas rough, angular particles provide a better degree of interlocking - inhibiting interparticle mobility – ultimately leading to a relatively higher frictional strength. Under the same conditions, at particle contact interfaces, angular particles must overcome greater frictional forces, before sliding can commence (Janoo 1998). A similar finding, observed by Shin & Santamarina (2013), stemmed from an increase in the mass fraction of angular particles in a sand mixture (comprising round and angular particles) that correlated to an increase in the friction angle of the granular mixture.

Cho et al. (2006) examined the effects of particle shape on packing density and on the small-to-large strain of crushed and natural sands, using two databases comprising published and new experimental data. Cho et al. (2006) explored and

presented correlations between index properties (sphericity, roundness, and regularity) and different mechanical properties influenced by particle shape. An increase in particle angularity and irregularity (i.e. decrease in sphericity and roundness) correlated to:

- an increase in the minimum and maximum void ratios, accompanied by an increase in the difference of extreme void ratios ($e_{max} - e_{min}$)
- an increase in the compressibility index, C_c, (under zero-lateral strain loading).
- a reduction in small-strain stiffness, coupled with increased sensitivity to the state of stress.
- an increase in the critical state friction angle

Moreover, irregular and angular particles promote a lower coordination number (i.e. average number of contact points between soil particles) and looser packing states (Santamarina & Cho 2004, Cho et al. 2006).

The quantitative assessment of particle shape descriptors has enhanced our understanding of the influence of shape on the mechanical behaviour of granular matter. According to Cho et al. (2006), each scale-dependent particle shape parameter "…*reflects aspects of the formation history and participates in determining the global behaviour of the soil mass from particle packing to mechanical response*". This sentiment underpins the basis of this work to reasonably measure and characterise particle shape using focus variation microscopy principles and evaluate its effect on the behaviour of sand in simple shear, particularly the response of contractive and dilative sand-sized specimens having contrasting form, angularity and roughness.

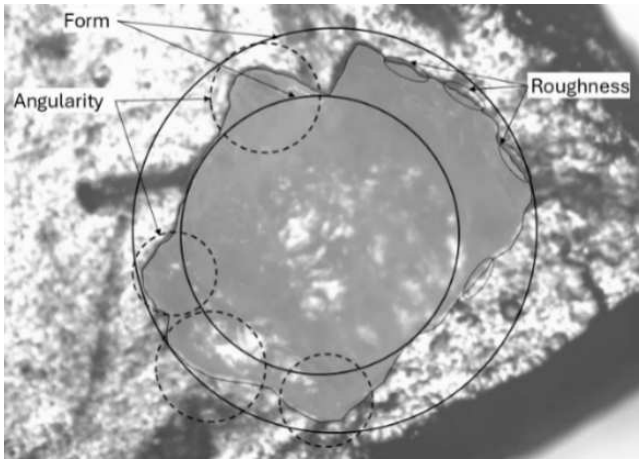

Figure 1. A silica sand particle indicating shape descriptors

2 MATERIALS AND METHODS

2.1 *Material types*

Material properties of the two material types are listed in Table 1. Silica sand (Fig. 2a) is a commercial crushed sand typically used in glass manufacturing, construction and water filtration. The glass beads (Fig. 2b) are commonly used in reflective paints, retroreflective road markings and abrasive blasting. Particle size distributions for both materials are shown in Figure 3. According to Bezuidenhout et al. (2024), the silica sand used in this experiment exhibits a high variability in form (Fig. 4), with particles ranging from discoid, platy, rod-like to equant, according to Zingg's (1935) form classes, whereas spherical glass beads were generally equant (Fig. 4).

Table 1. Index properties of materials used in this experiment

Parameter	Material type	
	Silica sand	Glass beads
Specific gravity G_s	2.67	2.52
Median particle size D_{50} (mm)	0.195	0.267
Coefficient of uniformity C_u	2.3	1.3
Coefficient of curvature C_z	1.1	1.0

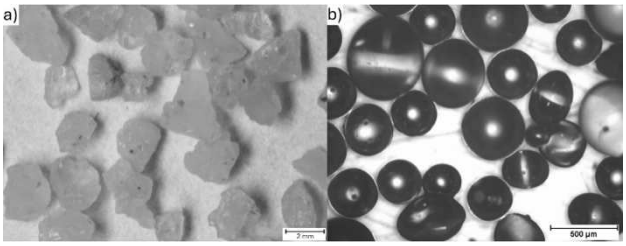

Figure 2. Micrographs of a) silica sand and b) glass beads

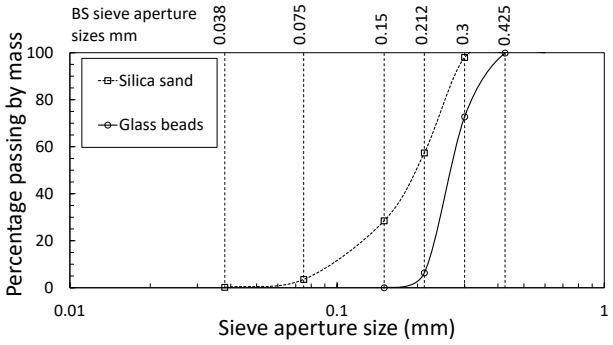

Figure 3. Particle size distribution of a) silica sand and b) glass beads

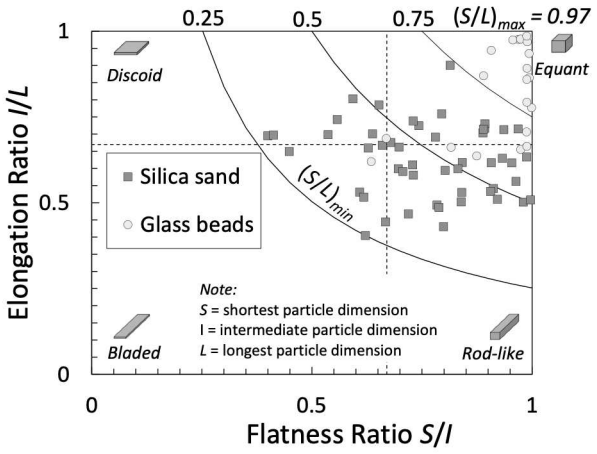

Figure 4. Particle form variability plotted on a Zingg diagram for a) silica sand and b) glass beads (from Bezuidenhout 2023)

2.2 *Experimental setup*

Table 2 describes the simple shear experimental programme. Constant volume direct simple shear tests, guided by ASTM 6528-07, were performed using a Geocomp ShearTrac II device to measure the undrained shear strength of the specimens prepared for this experimental programme. Loose silica sand (SS) specimens were prepared using wet pluviation whereas dense specimens were prepared using moist tamping. To achieve saturation, specimens were flushed, at a low pressure, using distilled water from an automatic pressure controller typically used in triaxial testing. Loose glass bead (GB) specimens were prepared using dry pluviation while dry tamping was adopted in dense GB specimens. A difference in the preparation techniques were adopted because the GB specimens achieved saturation significantly quicker in the Shear Trac II bath than SS specimens due to a coarser gradation. Dense GB specimens were also flushed to achieve saturation. The degree of saturation S was typically ~1, which was indirectly determined following ASTM 6528-07.

Table 2. The CVSS experimental programme

Test no.	Final vertical effective consolidation stress σ'_{v0}	Material type: e_0	
		Silica sand: test series (a)	Glass beads: test series (b)
1	100 kPa	1.12	0.96
2	200 kPa	1.12	0.95
3	300 kPa	1.11	0.93
4	100 kPa	0.73	0.68
5	200 kPa	0.71	0.68
6	300 kPa	0.75	0.68

Note: e_0 = preparation void ratio
Loose specimens: Tests no. 1 to 3. Dense: Tests no. 4 to 6.
CVSS = constant volume simple shear (undrained)

2.3 *Assessments of particle shape: angularity*

The current work evaluates angularity descriptors of 10 particles of each material type by measuring particle geometry from static micrographs, captured using a conventional optical microscope, with a limited depth of field, fitted with a complementary metal oxide semiconductor that digitised the field of view. Focus variation microscopy principles, described in Bezuidenhout et al. (2024), were adopted to assess particle outline under a microscope's objective. Particle geometry data, from Bezuidenhout et al. (2024), of 10 particles from the same material types, were also included in this paper to increase the size of the dataset and, therefore, improving its statistical representativeness. The current work assesses 2D descriptors assessed along the plan view of all particles.

Firstly, particle regularity ρ was computed using Wadell's (1932) roundness R and sphericity S, which further aided particle shape characterisation using a chart proposed by Krumbein & Sloss (1963). Regularity ρ is defined as:

$$\rho = \frac{R+S}{2} \tag{1}$$

$$R = \frac{\sum \frac{r}{r'}}{N} \tag{2}$$

$$S = \frac{r'}{r_{min-cir}} \tag{3}$$

where r = radius of curvature of a corner along the particle's outline; r' = radius of the maximum inscribed circle within the particle's outline; N = number of corners; $r_{min\text{-}cir}$ = minimum circumscribed circle along the particle's outline

Wadell's (1932) roundness procedure is time consuming and is beset with ambiguities on how to interpret a corner (Janoo 1998, Blott & Pye 2008, Le Pen et al. 2013). To evade these challenges and expedite angularity assessments, the ellipseness E parameter was adopted following Le Pen et al. (2013). Like Wadell's roundness, E is also based on a 2D projection of a particle and is defined as

$$E = \frac{P_e}{P_0} \qquad (\mathrm{E} \leq 1) \tag{4}$$

where P_0 is the particle perimeter, and P_e is the perimeter of an ellipse with an area (A) equal to the area of the 2D projection of the particle, and a major axis a equal to half of the length of the longest line joining two points on the particle perimeter and passing through its centroid of area. It is understood that E approaches a maximum value of 1 as the particle outline becomes more ellipse-like. Due to a lack of a closed form solution for the perimeter of an ellipse P_e, Le Pen at al. (2013) used the approximation presented in Equation 5 which was originally proposed by Ramanujan (1914).

$$P_e \approx \pi(a+b)\left(1 + \frac{3\left(\frac{a-b}{a+b}\right)^2}{10+\sqrt{4-3\left(\frac{a-b}{a+b}\right)^2}}\right) \tag{5}$$

where b ($=A/\pi a$) is the minor axis of the ellipse.

This work further explores correlations between particle shape descriptors and strength parameters defined by compressibility, shear strength and stiffness of material types subjected to consolidated undrained simple shear tests.

2.4 *Assessment of mechanical behaviour*

To simulate undrained shearing after consolidation, the Shear Trac II apparatus was configured to apply a vertically controlled load which helps maintain a constant specimen height during shearing. Moreover, Teflon coated rings help maintain constant volume conditions, as each specimen is sheared at a rate of approximately 0.2 mm/min. Soil behaviour was assessed as follows:

a) Compressibility was calculated using vertical displacements recorded by a linear-variable differential transducer during consolidation of the specimens, ranging between 100 and 300 kPa.
b) Due to a non-uniform shear stress distribution across the sample's cross-sectional area, an average shear stress was computed as follows:

$$\tau = \frac{F}{A} \quad (6)$$

where F = applied shear force; A = specimen cross-sectional area

c) During constant volume shearing, the magnitude to which the apparatus automatically adjusted the vertical stress to maintain a constant specimen height depended on the tendency of the specimen to contract or dilate - causing shear induced pore pressure ΔUs, defined as:

$$\Delta U_s = \sigma_{ps} - \sigma_v \quad (7)$$

where σ_{ps} = vertical consolidation stress at the start of shearing; σ_v = applied vertical stress

d) The undrained secant shear modulus G was estimated using Equation 8:

$$G = \left(\frac{\tau - \tau_{ps}}{\gamma}\right) x\ 100 \quad (8)$$

where τ = shear stress; τ_{ps} = shear stress at the start of shearing; γ = shear strain

3 RESULTS AND DISCUSSIONS

3.1 *Assessments of particle angularity*

Wadell's roundness distinguishes well between rounded and angular particles (Fig. 5a). Despite varying over a narrow range (0.83 < E < 1), E differentiates angular and rounded particles better than S (Fig. 5b). The effect of including R in the definition of regularity ρ causes a significant downward shift of the entire dataset as shown in Figure 5c. These observations indicate that the definition of S adopted is representative of particle form (i.e. an aspect ratio) and not angularity.

Table 3 provides a summary of basic R and E statistical parameters. R varies over a broader range and separates the rounded and angular particles significantly better than both S and E.

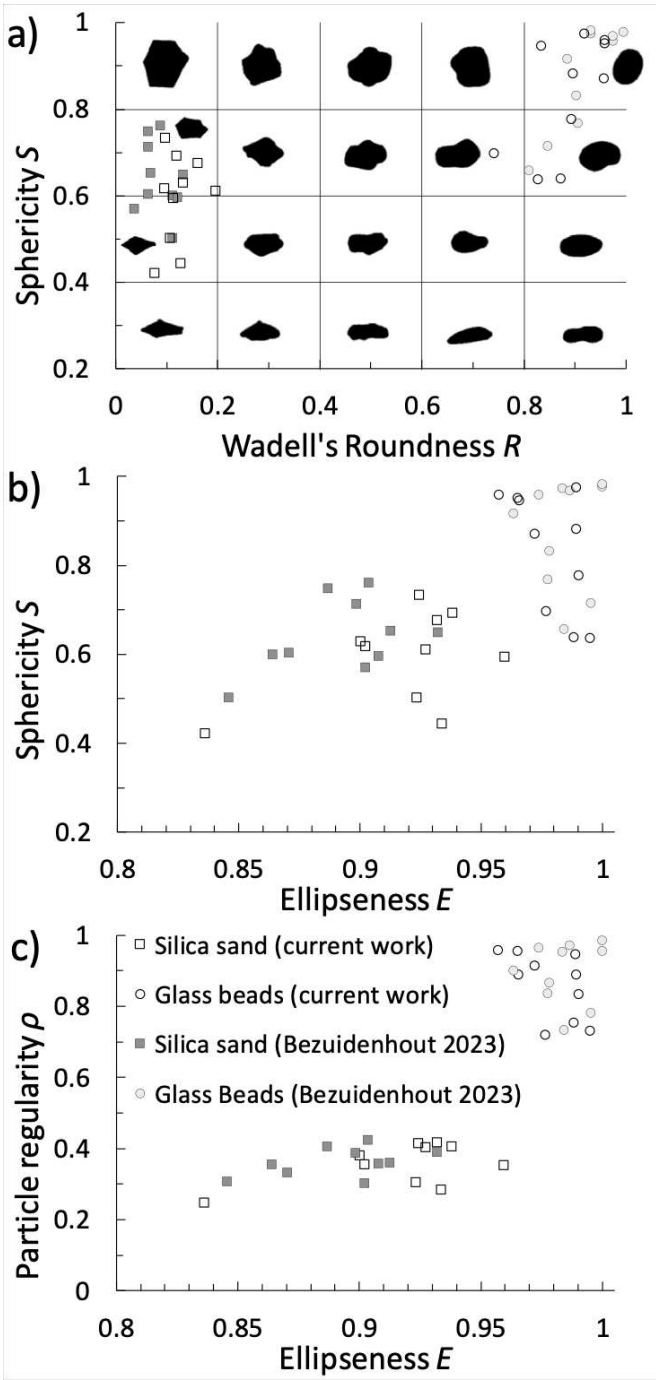

Figure 5. Shape characterisation a) roundness R vs sphericity S (after Krumbein & Sloss 1963), b) ellipseness E vs sphericity S, and c) ellipseness E vs regularity ρ

Table 3. The direct simple shear experimental programme

Angularity descriptor	Statistical parameter	Material type	
		Silica sand (SS)	Glass beads (GB)
Wadell's Roundness R	Mean	0.11	0.90
	Standard deviation	0.04	0.06
	Minimum	0.04	0.74
	Maximum	0.20	0.99
Ellipseness E	Mean	0.91	0.98
	Standard deviation	0.03	0.01
	Minimum	0.84	0.96
	Maximum	0.96	1

3.2 *Assessment of compressibility*

Figure 6 shows the compressibility results from tests 3a, 3b, 5a and 5b. The GB fabric is slightly more sensitive to initial deformability than SS (Fig. 6a and 6b) – likely due to the ease at which contact slip can be mobilised at lower stresses along the smooth rounded particles. Despite a higher e_0, SS exhibits a higher mean compressibility of ~0.08 compared to ~0.05 yielded by GB between 50 and 300 kPa (Fig. 6a). Per Figure 6b, at approximately similar dense e_0, SS and GB exhibit a similar coefficient of compressibility C_c of ~0.04, between a σ_{v0}' of 25 and 75 kPa. Across 100 < σ_{v0}' < 200 kPa, SS produces a slightly higher C_c of 0.046, compared to 0.033 yielded by GB.

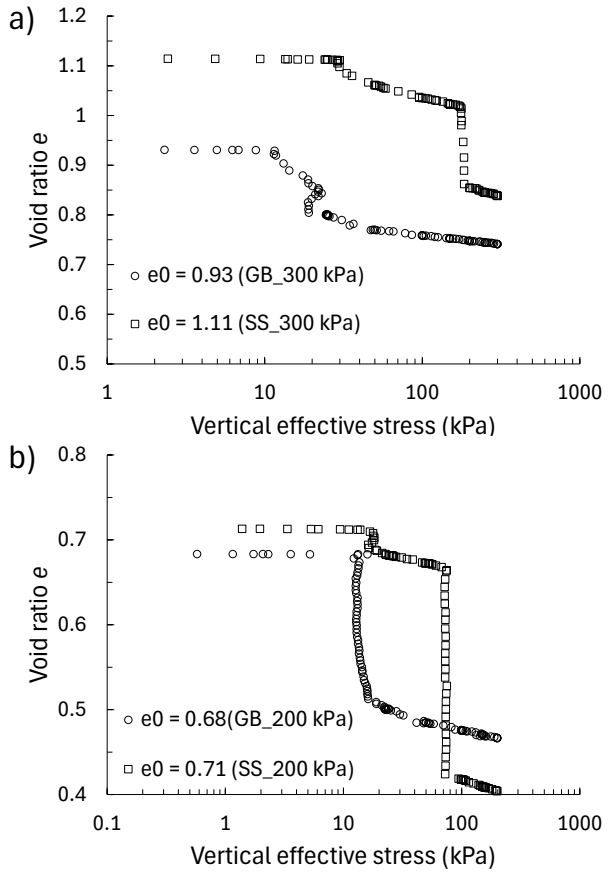

Figure 6. Consolidation results of silica sand and glass beads a) loose specimens, σ_{v0}' = 300 kPa and b) dense specimens, σ_{v0}' = 200 kPa

3.3 *Assessment of undrained behaviour in shear*

At a contractive state, the undrained response of SS and GB, consolidated to a pre-shear stress of 100 kPa, are largely undistinguishable, whereas the σ_{v0}' of 200 and 300 kPa tests follow a similar respective trend, as shown in Figure 7a and 7b. That is, the shear stress response curves plot close to another from the approach to an initial peak at 0% < γ < 3% until γ = 50%. For σ_{v0}' of 100 and 200 kPa, the initial shear stress peaks suddenly reduce due to a buildup of positive shear induced pore pressure that appears to monotonically increase but fluctuates noticeably after γ > 20%. It is unclear what causes the fluctuation, which is appreciably greater in GB tests, in the ΔU_s response; the effect of a non-uniform shear stress distribution may be a contributing factor of this pattern, but this warrants further investigation. For σ_{v0}' = 300 kPa, the effect of increasing the consolidation stress, causes a higher second peak when 29% < γ < 35%, and a tendency of both SS and GB to dilate as observed by the reduction in ΔU_s over this γ range.

Despite, the lower e_0 in GB specimens (due to spherical particles promoting a higher coordination number), dense SS specimens yield higher a shear strength (Fig. 7c). It is hypothesised that during shearing of a dense soil fabric, the tendency of individual irregular and angular shaped particles to mobilise to rotate and translate relative to another is significantly more difficult compared to smooth, rounded spherical particles – resulting in an increased shearing resistance. In addition to this effect, when volume change is restricted during CVSS tests, the tendency for the SS fabric (comprising irregular and angular shaped particles) to promote a looser packing (i.e. volume increase), draws pore water into the spaces the particles are trying to vacate. Because constant volume conditions prevent this behaviour from occurring, greater effort is imparted by the test apparatus applying the normal stress – increasing the shear stress.

Furthermore, in dense specimens, SS yields slightly lower undrained secant shear moduli at low γ typically < 1.5% - due to SS having a relative more compressible fabric at small strains. After the onset of dilation, the reduction in undrained stiffness is significantly higher in spherical GB than angular SS, due to a lower degree to which its fabric dilates.

In all shear tests, the response of GB is noticeably jagged, which may be attributed to the tendency of the contact slippage and suboptimal grip between the steel pins at the soil-load platen interfaces.

3.4 *Correlating particle shape to mechanical behaviour*

Compressibility decreases with increasing roundness and regularity as shown in Figure 8a. These results agree with findings reported in Cho et al. (2006) and data re-plotted from Santamarina & Cho (2004). In natural sands, compressibility decreases considerably with increasing regularity. As shown in Figure 8b, a correlation between the mean undrained secant shear modulus G and R is performed at large shear strain (when $\gamma \approx 40\%$ at the peak of dilation) because G becomes largely distinguishable between the two material types and produces an almost linear slope on a log(G) vs log(γ) plot, when 40% < γ < 55% in all tests. Angular SS exhibits a higher G at large shear strain due to the onset of dilation.

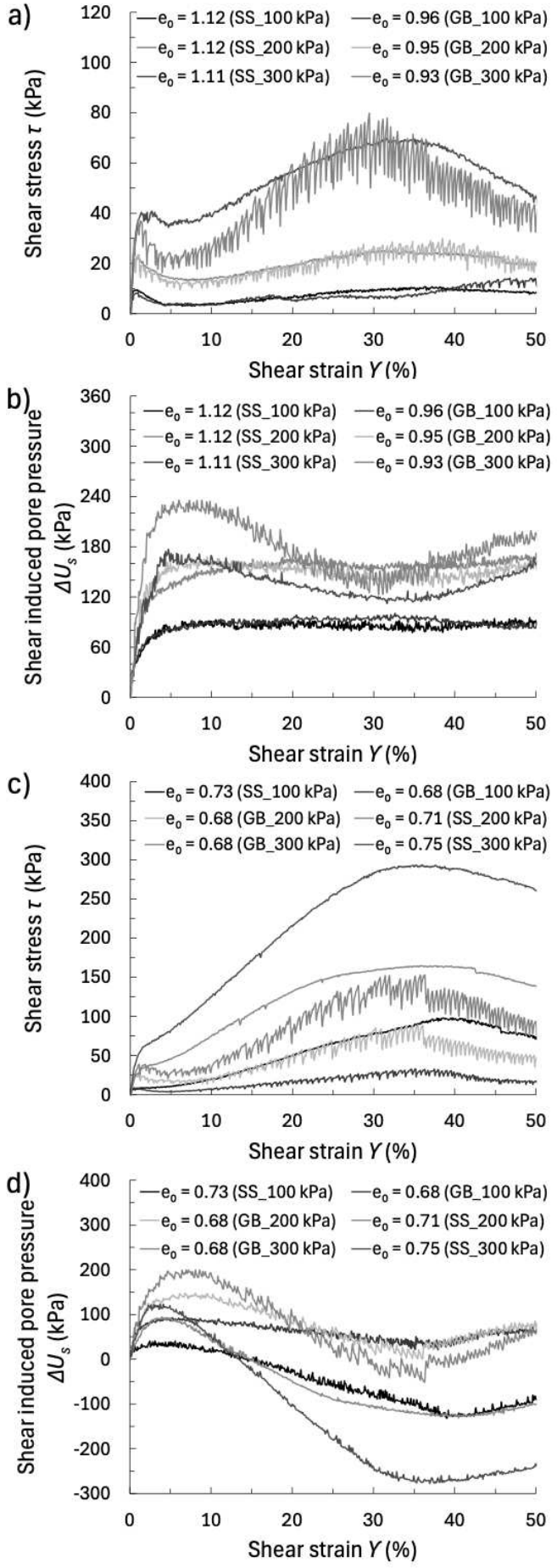

Figure 7. CVSS test results of SS and GB, loose specimens: a) τ vs γ b) ΔU_s vs γ, and dense specimens: c) τ vs γ and d) ΔU_s vs γ

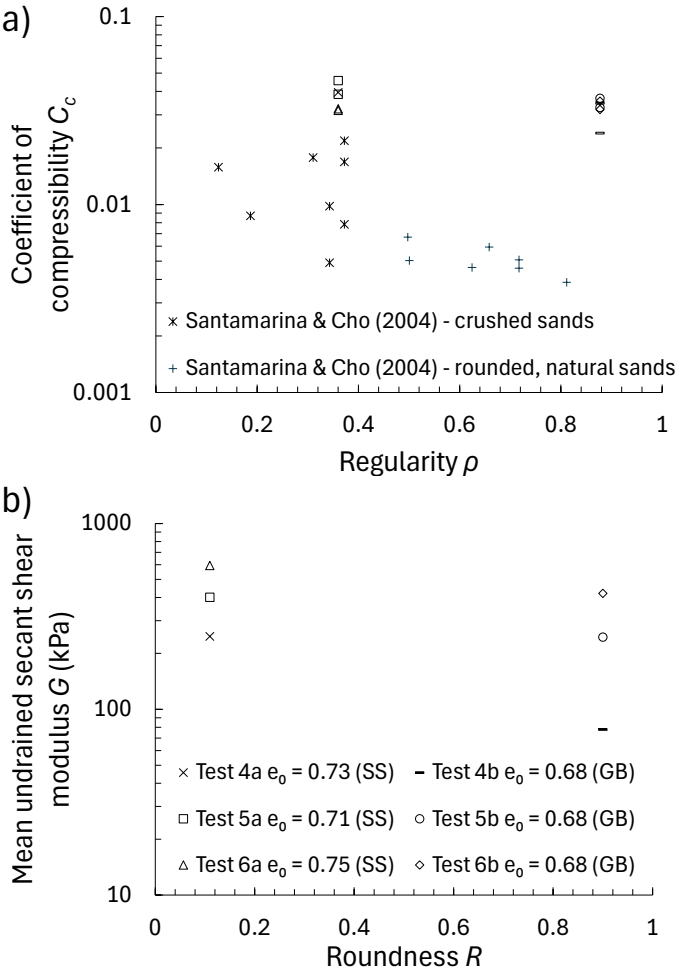

Figure 8. Correlation between a) C_c and R b) C_c and R

4 CONCLUSIONS

This study investigated particle shape effects on the response of sand-sized particles in constant volume direct simple shear. Particle shape descriptors were determined using focus variation microscopy-based principles. The study reports the following findings:

a) In spherical glass beads, an increase in the jaggedness of the data is observed with increasing consolidation stress. This is attributed to contact slippage and suboptimal grip between both load platen-soil interfaces. Slippage is interpreted from the recurrent abrupt drops and increases in shear force at discrete shear strain magnitudes.
b) The more irregular shaped the soil particles, the greater the deformability. This is analogous to a cone-to-contact plane versus a sphere-to-contact plane (Goddard 1990).
c) In dense specimens, irregular particles promote dilation resulting in increased strength and undrained modulus during dilation.
d) The shear stress and undrained shear moduli are similar in magnitude and trend with increasing shear strain in both loose silica sand and glass beads - suggesting particle shape has minimal effect in a contractive soil fabric subjected to low

stresses – likely due to a lack of interparticle contact in loose specimens.

e) Like Cho et al. (2006), an increase in friction angle is observed with a decrease in soil regularity.
f) The effect of increasing soil density from a contractive to a dilative fabric is more distinct in the silica sand than glass beads - shown by the significant increase in friction angle, compressibility and large-strain undrained modulus - suggesting that angular particles have a more sensitive fabric.

For sands, the literature reports that particle shape affects index properties, compressibility, shear stiffness, drained and undrained shear strength and critical state parameters. Thus, this work's findings, in addition to those from the literature, warrant the need to include particle shape characterisation in standard soil classification guidelines for sands.

REFERENCES

ASTM D6528-07. 2007. *Standard Test Method for Consolidated Undrained Direct Simple Shear Testing of Cohesive Soils*. ASTM International.

Alshibli, K.A., Druckrey, A., Al-Raoush, R. & Weiskittel, T.M. 2014. Quantifying Morphology of Sands Using 3-D Imaging. *J. Mater. Civil Eng*.

Barret, P.J. 1980. The shape of rock particles: a critical review. *Sedimentology* 27(3): 291-303.

Bezuidenhout, A.W. 2023. Shape characterization of coarse particulates aided by focus variation microscopy. Research report for the degree of Master of Science in Engineering. University of the Witwatersrand, South Africa.

Bezuidenhout, A.W., Bodhania, M., Tiroyabone, L., Eddey, C. & Torres-Cruz, L.A. 2024. The shape of sand particles: Assessments of three-dimensional form and angularity. *Soils and Foundations* 64(1).

Blott, S. & Pye, K. 2008. Particle shape: a review and new methods of characterization and classification. *Sedimentology* 55: 31-63.

Cho, G., Dodds, J. & Santamarina, J. 2006. Particle shape effects on packing density stiffness and strength: natural and crushed sands. *J. Geotech. Environ. Eng*. ASCE 132(5): 591-602.

Clayton, C.R.L., Abbireddy, C.O.R. & Schiebel, R. 2009. A method of estimating the form of coarse particulates. *Geotechnique* 59(6): 493-501.

Goddard, J.D. 1990. Nonlinear elasticity and pressure-dependent wave speeds in granular media. Proc. R. Soc. London, Ser. A 430: 105-131.

Holtz, R.D. & Kovacs, W.D. 1981. *An Introduction to Geotechnical Engineering*. Englewood Cliffs, New Jersey: Prentice-Hall Inc.

Janoo, V.C. 1998. Quantification of Shape, Angularity, and Surface Texture of Base Course Materials.

Krumbein, W.C. & Sloss, L.L. 1963. *Stratigraphy and sedimentation*. San Francisco: Freeman and Company.

Le Pen, L.M., Powrie, W., Zervos, A., Ahmed, S. & Aingaran, S. 2013. Dependence of shape on particle size for a crushed rock railway ballast. *Granular Matter* 15: 849-861.

Ramanujan, S. 1914. Modular equations and approximations to π. Q. *J. Pure ppl. Math*. 45: 350-372.

Santamarina, J.C. & Cho, G.C. 2004. Soil Behavior: The Role of Particle Shape. Conference on Advances in Geotechnical Engineering, London: 604-617.

Shin, H. & Santamarina, J.C. 2013. Role of particle angularity on the mechanical behaviour of granular mixtures. *J. Geotech. Geoenviron*. 139: 353-355.

Wadell, H. 1932. Volume, shape and roundness of rock particles. *J. Geol*. 40: 443-451.

Wang, X., Wu, Y., Cui, J., Zhu, C. & Wang, X. 2020. Shape Characteristics of Coral Sand from the South China Sea. *Journal of Marine Science and Engineering* 10(8).

Zhao, B., Wang, J., Coop, M.R., Viggiani, G., Jiang, M. 2015. An investigation of single sand particle fracture using X-ray micro tomography. *Géotechnique* 65(8): pp. 625-641.

Zhou, B., Wang, J. & Wang, H. 2017. Three-dimensional sphericity, roundness and fractal dimension of sand particles. *Géotechnique* 68(1): 18-30.

Zingg, T. 1935. Beitrage zur Schootteranalyse. Schweizminer. *Petrog. Mitt*. 15: 38-140.